

Polyamorphism of GeO₂ Glass at High Pressure

Xinguo Hong* and Matt Newville

HPSTAR
933-2020

Polyamorphism of network-forming SiO₂ and GeO₂ glasses at high pressures is a puzzling topic in condensed matter physics and has long-standing interest because of their important geophysical and geochemical implications. Molecular dynamics simulations suggest that there are multiple amorphous–amorphous transitions at high pressure with parallel high-pressure crystalline counterparts. However, it is very challenging to experimentally distinguish the pressure-induced subtle change in the amorphous state at high pressure. Recently, a high-pressure X-ray absorption fine structure (HP-XAFS) method is developed using a diamond anvil cell (DAC) to measure the local structure of polyamorphs in GeO₂ glass at high pressure. The results indicate that GeO₂ glass shows multiple polyamorphs at high pressure with a local structure, in general, similar to their high-pressure crystalline states in the first coordination shell but with increasing differences in the distant coordination shells. Three pressure-induced polyamorphs in GeO₂ glass are recognized unambiguously at high pressure, i.e., α -quartz-like, rutile-like, and pyrite-like amorphous structures. The obtained knowledge of these polyamorphs is helpful for understanding the mechanisms of network compression behavior and physical properties of SiO₂ and GeO₂ glasses and melts under extreme conditions.

absorption fine structure (XAFS) and X-ray total scattering experiments further provide the evidences of rutile-like GeO₂ glass^[10] and pyrite-like GeO₂ glass.^[11] However, despite previous successful investigations, a detailed understanding of the pressure-induced polyamorphs is still lacking.^[1,4–6,9] For example, open questions remain on the existence of multiple octahedral polyamorphs under extreme conditions of high pressure and temperature and how to distinguish/characterize the subtle amorphous states at ultrahigh pressures.^[9]

GeO₂ glass is regarded as an analog for the silica (SiO₂) glass and melt in the Earth's interior.^[1] It displays parallel compression behavior as SiO₂ glass but at lower accessible pressures. Moreover, GeO₂ glass is of particular interest, because the local structure of Ge atoms can be measured in situ by XAFS techniques in a diamond anvil cell (DAC), whereas it is impossible to carry out a high-pressure XAFS (HP-XAFS) experiment for SiO₂ glass due to the seri-

ous X-ray absorption of diamond anvils at Si or O K-edge.

It is well known that the XAFS technique is an effective tool to address the pressure-induced subtle polyamorphs of GeO₂ glasses under high pressure.^[7,10,12–14] It should be a perfect complementary tool to X-ray diffraction for high-pressure structure determination. However, due to the Bragg reflections from the diamond anvils, the XAFS spectra of GeO₂ glass at a high pressure feature many DAC-imposed glitches.^[14] The XAFS technique has long been regarded unsuitable for the DAC environment because of the significant absorption and diffraction effects of the diamond anvils.^[15] We have developed an iterative method able to obtain glitch-free XAFS data at high pressure.^[14] In this article, we present our results for the existence of multiple polyamorphs in the network-forming GeO₂ glass at high pressure with local structures in a certain degree of similarity to their high-pressure crystalline states.


1. Introduction

Pressure-induced structural changes of the “strong” network-forming SiO₂ and GeO₂ glasses have been extensively studied due to their importance in industry, materials, and geological sciences.^[1–7] In particular, the polyamorphous transition from tetrahedral to octahedral glasses is of great interest due to its geological importance in the Earth's mantle.^[8] At ultrahigh pressures, multiple postoctahedral amorphous–amorphous transitions, as their crystalline counterparts, are predicted by molecular dynamics simulations.^[9] Experimentally, X-ray

Dr. X. Hong
Center for High Pressure Science and Technology Advanced Research
Beijing 100094, P. R. China
E-mail: xinguo.hong@hpstar.ac.cn, xinguo.hong@gmail.com

Dr. X. Hong
Mineral Physics Institute
Stony Brook University
Stony Brook, NY 11794, USA

Dr. M. Newville
Consortium for Advanced Radiation Sources
University of Chicago
Chicago, IL 60637, USA

 The ORCID identification number(s) for the author(s) of this article can be found under <https://doi.org/10.1002/pssb.202000052>.

DOI: 10.1002/pssb.202000052

2. Results and Discussion

The structure of GeO₂ crystals is very useful for understanding the polyamorphs of GeO₂ glass, because a direct parallel between the amorphous and crystalline states has been predicted by molecular dynamics simulations.^[9] Recent XAFS and pair-distribution function (PDF) experiments also confirm this certain degree of parallels in GeO₂ glass to their crystalline counterparts under pressure.^[10,11] Figure 1 shows the k^2 -weighted

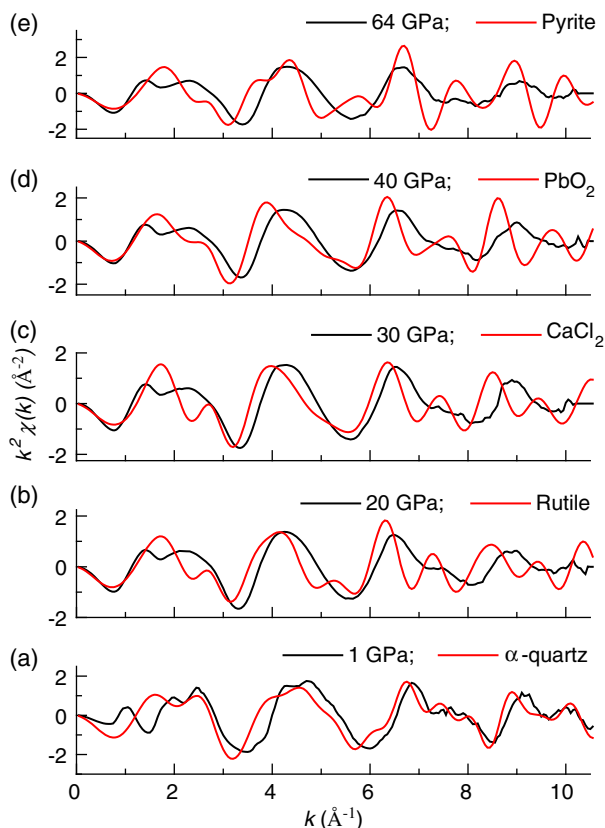


Figure 1. The k^2 -weighted XAFS spectra, $k^2\chi(k)$, for GeO_2 glass at high pressures. Solid black lines are the experimental XAFS data for GeO_2 glass at a) 1 GPa, b) 20 GPa, c) 30 GPa, d) 40 GPa, and e) 64 GPa. The red lines denote the crystalline counterparts at high pressures from FEFF calculations.^[16]

XAFS spectra, $k^2\chi(k)$, for GeO_2 glass at the pressures of 1 GPa (Figure 1a), 20 GPa (Figure 1b), 30 GPa (Figure 1c), 40 GPa (Figure 1d), and 64 GPa (Figure 1e), together with the theoretical spectra of the corresponding high-pressure crystalline structures using FEFF code.^[16] The α -quartz-like GeO_2 structure is taken from the study by Jorgensen.^[17] It is found that a proper damping on the theoretical FEFF spectra is necessary for a sound comparison. A Debye–Waller factor of 0.006 can result in overall good matching between the theoretical and experimental k^2 -weighted XAFS spectra for the α -quartz-like GeO_2 structure (Figure 1a). This factor is then applied to all other spectra at high pressures. As shown in Figure 1, the overall XAFS spectra of crystals and GeO_2 glass show basically good similarities in the oscillation profile, period, and amplitude at the respective pressures. It is notable that crystalline XAFS data show more features with better XAFS resolution.

Figure 2 shows the corresponding XAFS Fourier transform, $|\chi(R)|$, for GeO_2 glass at high pressures (Figure 1). The height of the first Ge–O peak of theoretical XAFS data is slightly different from that of the experiment but normalized to the respective experimental ones for comparison. It is clear that the first Ge–O coordination shell of GeO_2 glass shows remarkable similarities in the peak positions and profiles with those of crystalline counterparts, whereas a large difference occurs at high

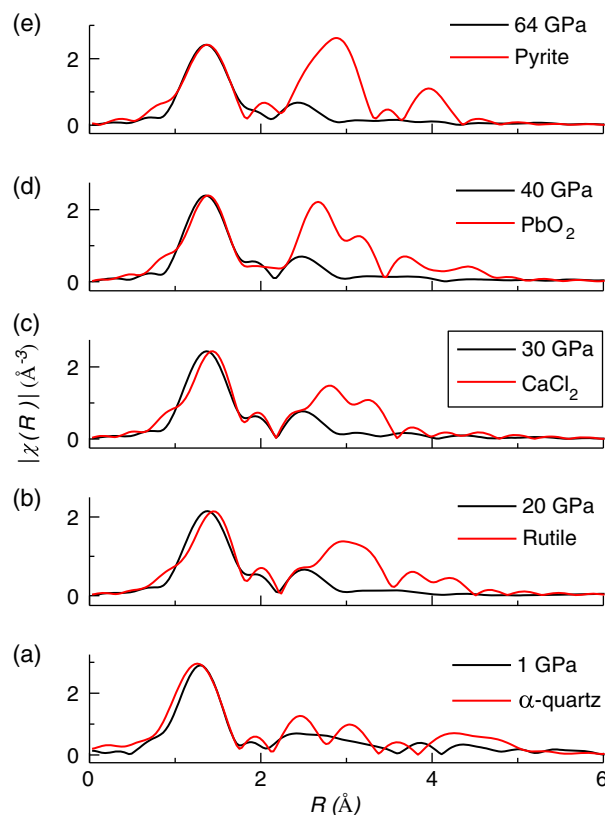


Figure 2. The corresponding XAFS Fourier transform, $|\chi(R)|$, for GeO_2 glass at high pressures. a–e) Notations are the same as Figure 1. Note the remarkable change at high coordination shells (2.2–3.5 Å, no phase correction).

coordination shells (2.2–3.5 Å, no phase correction). Thus, the predicted direct parallel between the pressure-induced amorphous and crystalline states^[9] is only valid in the nearest coordination shell. There is only a small difference for the octahedral glass (rutile, CaCl_2 , PbO_2 , and pyrite GeO_2). This feature is consistent with the recent measurement of X-ray emission spectroscopy, by which the octahedral glass is expected to persist up to the Mbar (100 GPa) range.^[18]

As shown in Figure 2, except the notable tetrahedral to octahedral transition, GeO_2 glass shows only subtle changes in the second peak (2.2–3 Å, no phase correction) at pressures above 20 GPa. In contrast, the XAFS data of octahedral crystalline structures show distinct changes in this second peak with splitting (CaCl_2 , 30 GPa) and merging (Pyrite, 64 GPa), as pressure increases. This change is, however, hard to be traced from the XAFS experiment (Figure 2).

At a low pressure, the overall profile of XAFS data at 1 GPa is in good agreement with that of the α -quartz-like GeO_2 structure (Figure 2). Many existing works^[5,6,19–23] have demonstrated the noteworthy similarities in the tetrahedral coordination number and distance between amorphous and crystalline GeO_2 . It is necessary to check the similarities in the clusters of tetrahedral GeO_2 glass with that of the tetrahedral crystalline structure beyond the tetrahedral GeO_4 units. **Figure 3** shows the α -quartz-based structural modelling to the Fourier transformation modulus, $|\chi(R)|$,

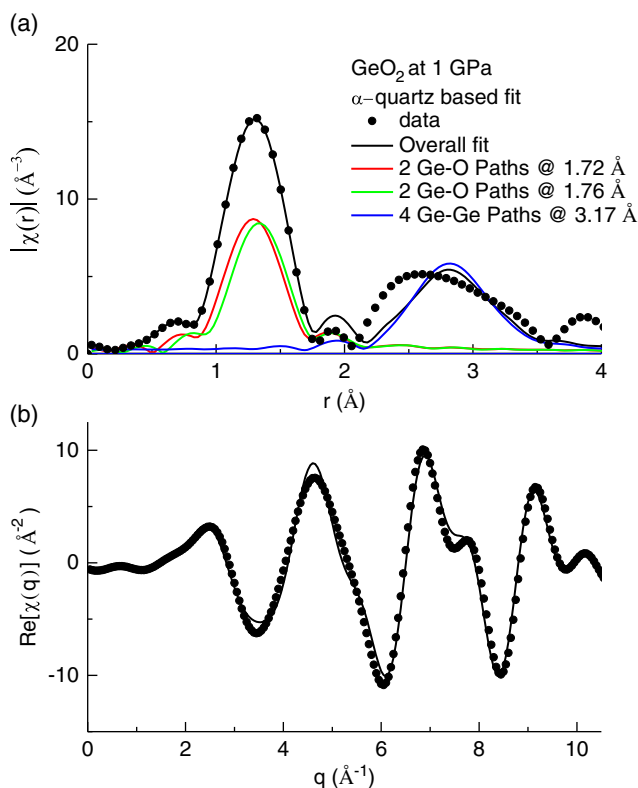


Figure 3. Structural modelling based on the cluster of α -quartz-like GeO_2 at 1–3 Å. a) Fourier transformation modulus, $|\chi(R)|$, of $k^2\chi(k)$ for GeO_2 glass at 1 GPa (full circles). The α -quartz-like structural modelling (black line) contains a tetrahedron of two O atoms at 1.72 Å (red line) and other two at 1.76 Å (green line). The four Ge atoms is located at 3.17 Å (blue line). b) A comparison of back-transformed $|\chi(R)|$ at 1–3 Å between experimental data (full circles) and best-fit calculation (black line) in q -space.

of $k^2\chi(k)$ for GeO_2 glass at 1 GPa in the range of 1–3 Å. It gives a decent fitting with a goodness-of-fit parameter, R_w , of 2.4%. To keep the integrality of the pyrite structure, no change on the path degeneracies and relative amplitude, the same distance variables were used for each coordination shell. This cluster fitting (black line) results in a tetrahedral GeO_4 unit consisting of two O atoms at 1.72 Å (red line) and other two at 1.76 Å (green line). The four Ge atoms locate at 3.17 Å (blue line). As shown in the real space (Figure 2a) and in the q -space (Figure 2b), the cluster of α -quartz structure at 1–3 Å can be well persisted in the amorphous state. The nearest Ge–O bond distance elongates by 0.01 Å, whereas that of Ge–Ge distance is 0.02 Å between GeO_2 glass at 1 GPa and α -quartz-like GeO_2 crystal at ambient.^[17] This cluster fitting supports the conclusion of tetrahedral GeO_2 glass at a low pressure.

The rutile-like GeO_2 glass was first reported by XAFS and X-ray total scattering experiments.^[10] Figure 4 shows a comparison between XAFS and X-ray total scattering in the Ge–O coordination in real space for GeO_2 glass at 20 GPa (black line), together with theoretical XAFS data of rutile-like GeO_2 (red line) by FEFF calculations.^[16] The pair-distribution function, $g(r)$, of the X-ray total scattering experiment^[10] is shifted by a constant of -0.42 Å for a direct comparison with the XAFS data without

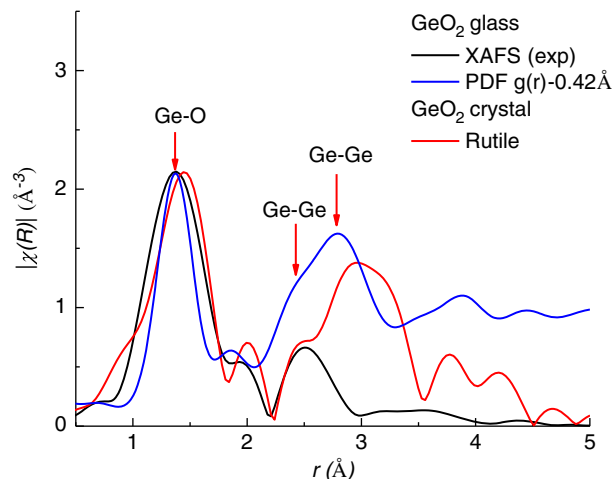


Figure 4. A comparison of XAFS Fourier transform $|\chi(R)|$ for GeO_2 glass at 20 GPa (black line) with the theoretical FEFF data of rutile-type GeO_2 (red line)^[16] and the pair-distribution function, $g(r)$, from the X-ray total scattering experiment.^[10] The data $g(r)$ are shifted by -0.42 Å for a direct comparison with the XAFS data (no phase correction).

further phase correction. All the data show good consistency in the first Ge–O coordination shell and the short Ge–Ge peak position at 2.34 Å (no phase correction) or 2.76 Å.^[10] The longer Ge–Ge distance at 2.81 Å (no phase correction) or 3.23 Å in the unshifted $g(r)$ function only shows a weak contribution to the XAFS coordination distribution, $|\chi(R)|$, as evidenced by the asymmetric shape of the second peak in $|\chi(R)|$. The theoretical XAFS data agree well with the $g(r)$ data in this long Ge–Ge bond distance (Figure 4). This illustrates that the XAFS technique is a local structural tool for structural analysis and has limitations for high coordination shells. As shown in Figure 4, the background of $g(r)$ function is much higher than XAFS data due to the total scattering contributions of all atomic pairs. The exact coordination shell in $g(r)$ function is hard to be separated beyond the first coordination shell. It is reported to be quite difficult to distinguish the penetration of O–O distribution into the first coordination shell in the X-ray diffraction experiment^[24] and theoretical simulations,^[25] which may result in overestimation of the Ge–O coordination number, i.e., a debate on the so-called fake ultrahigh amorphous state.^[18] In contrast, the XAFS technique has an obvious advantage due to the unique capability of atomic resolution. In results, as shown in Figure 4, we need both XAFS (local tool) and X-ray total scattering diffraction (average structure) for a comprehensive understanding of the structural similarity between amorphous and crystalline structures.

We have shown the existence of pressure-induced α -quartz-like (Figure 3) and rutile-like (Figure 4) amorphous state GeO_2 glass. However, it would be extremely challenging to demonstrate the existence of other octahedral CaCl_2 -like or PbO_2 -like amorphous states in GeO_2 glass because of the similar profiles in coordination shells (Figure 2). This subtle difference calls for some advanced high-resolution X-ray total scattering and XAFS experiments to probe these amorphous states in the future. Beyond the PbO_2 -like crystalline state, the pyrite-like structure

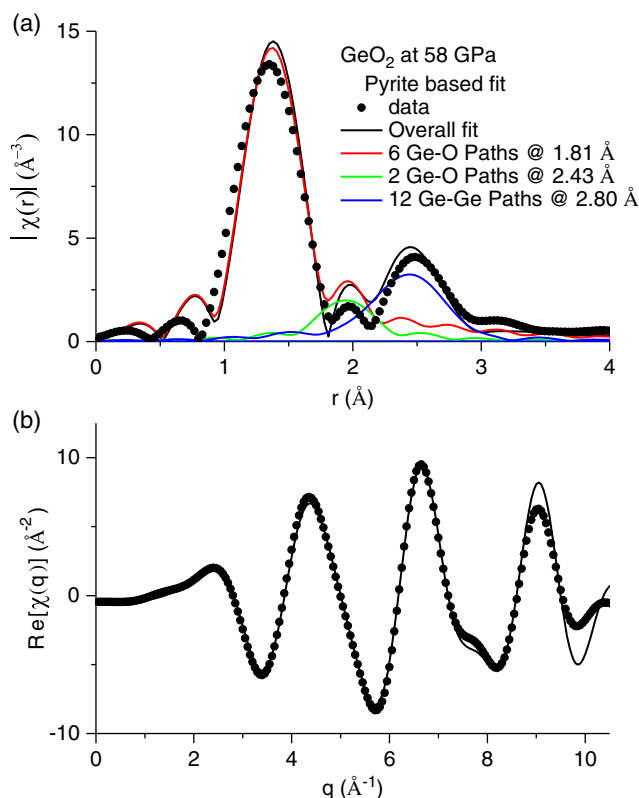


Figure 5. Structural modelling based on the cluster of pyrite-like GeO_2 at 1–3 \AA . a) Fourier transformation modulus, $|\chi(r)|$, of $k^2\chi(k)$ for GeO_2 glass at 58 GPa (full circles). The pyrite-based structural modelling (black line) yields 6 O atoms at 1.81 \AA (red line), 2 distant O atoms at 2.43 \AA (green line), and 12 Ge atoms at 2.80 \AA (blue line). b) A comparison of back-transformed $|\chi(r)|$ at 1–3 \AA between experimental data (full circles) and best-fit calculation (black line) in q -space.

is the next stable state in the GeO_2 crystal.^[26] The pyrite-like amorphous state was reported to exist at 64 GPa in GeO_2 glass.^[11]

Figure 5 shows a pyrite-based structural modelling for GeO_2 glass at a slightly lower pressure. The cluster modelling is based on the pyrite local structure in the range of 1–3 \AA for GeO_2 glass. It gives a good fitting for the XAFS spectra at 58 GPa with a decent goodness-of-fit parameter, R_w , of 2%. To keep the integrality of the pyrite structure, no change on the path degeneracies and relative amplitude, the same distance variables were used for each coordination shell. This pyrite-based cluster fitting (black line) yields 6 O atoms at 1.81 \AA (red line), 2 distant O atoms at 2.43 \AA (green line), and 12 Ge atoms at 2.80 \AA (blue line). The structural fitting using the pyrite-like cluster is shown in the real space (Figure 5a) and in the q -space (Figure 5b). The value of R_w is slightly worse than that of 0.6% for structural modelling of the pyrite-like structure for GeO_2 glass at 64 GPa,^[11] but we can conclude that the pyrite-like amorphous structure is largely formed in GeO_2 glass at 58 GPa.

In comparison with the pyrite-like GeO_2 crystalline structure in detail,^[26] the GeO_2 glass at 58 GPa shows a small difference in the nearest Ge–O distance with an elongation of 0.03 \AA (bond, red line) but an increasing deviation at the distant Ge–O distance of -0.14 \AA (bond, green line). Significant deviation is found in

the Ge–Ge distance as large as -0.27 \AA in GeO_2 glass at 58 GPa in comparison with the crystalline structure.^[26] Such an increasing deviation as a function of the coordination distance holds true for the α -quartz-like (Figure 3), rutile-like (Figure 4), and pyrite-like (Figure 5) GeO_2 glasses. Thus, the certain degree of parallel between the pressure-induced amorphous and crystalline states^[9] is valid only for the nearest coordination shell, but the amorphous state has its own compaction mechanism at higher coordination shells.

3. Conclusions

We have shown that the structure of GeO_2 glass has high similarities with the crystalline counterparts in the nearest coordination shell at high pressure. At least, three distinct polymorphs in GeO_2 glass at high pressure, i.e., α -quartz-like, rutile-like, and pyrite-like structures, have been recognized unambiguously. The obtained knowledge of these polymorphs is useful for understanding the mechanisms of network compression and corresponding property changes in SiO_2 and GeO_2 glasses and melts under extreme conditions.

4. Experimental Section

GeO_2 glass samples were made by quenching GeO_2 melt at 1600 $^\circ\text{C}$ (donated by L. Huang at Rensselaer Polytechnic Institute, New York). Symmetrical DACs with normal single-crystalline diamond anvils were used in the experiments. Ruby chips were placed at the edge of sample chamber for pressure determination using the ruby fluorescence technique.^[27] XAFS experiments were conducted on the Ge K-edge of the glass in transmission mode at the GeoSoilEnviroCARS bending magnet beamline 13-BM-D, Advanced Photon Source (APS), Argonne National Laboratory. XAFS spectra were collected from 10 953 to 11 747 eV with 5 eV steps before the main edge, with 0.5 eV steps from -10 to 25 eV across the main edge (11 110 eV), and with 0.05 \AA^{-1} steps in k -space to 13 \AA^{-1} above the main edge. An iterative method was used to progressively identify and eliminate the DAC glitches at a set of multiple angles.^[14] The method provides high-quality, glitch-free XAFS spectra above the Ge K-edge by 410 eV ($k = 10.4$ \AA^{-1}). Further XAFS data processing and analysis were then performed with the ATHENA and ARTEMIS programs^[28] of the IFEFFIT package.^[29] Other experimental details are described previously.^[11,14]

For comparing the structural similarity between GeO_2 amorphous and crystalline states, we have to obtain the theoretical structure at the same pressures as the XAFS experiments. Density functional theory calculations were carried out to optimize the corresponding GeO_2 crystalline structures at the experimental pressures using the Perdew–Burke–Ernzerhof (PBE)-type generalized gradient approximation (GGA)^[30] implemented in the QUANTUMESPRESSO code.^[31] Scalar relativistic ultrasoft pseudopotentials (Ge.pbe-n-rrkjus_psl.1.0.0.UPF and O.pbe-rrkjus.UPF) were used in the calculation of the structural optimization of crystalline GeO_2 at high pressure. Both the lattice parameters and Wyckoff positions of atoms were optimized.

Acknowledgements

The authors thank L. Huang, T. Lanzirrotti, X. M. Yu, and N. Lazarz for their assistance with the experiments. The Center for High Pressure Science and Technology Advanced Research is supported by the National Natural Science Foundation of China (U1530402). The GSECARS sector of APS is supported by NSF (EAR-1128799) and DOE (DE-FG02-94ER14466).

Conflict of Interest

The authors declare no conflict of interest.

Keywords

density functional theory, glasses, high pressures, X-ray absorption fine structure

Received: January 24, 2020

Published online:

- [1] M. Micoulaut, L. Cormier, G. S. Henderson, *J. Phys.: Condens. Matter* **2006**, 18, R753.
- [2] A. C. Wright, *J. Non-Cryst. Solids* **1994**, 179, 84.
- [3] D. L. Price, M.-L. Saboungi, A. C. Barnes, *Phys. Rev. Lett.* **1998**, 81, 3207.
- [4] J. P. Itie, A. Polian, G. Calas, J. Petiau, A. Fontaine, H. Tolentino, *Phys. Rev. Lett.* **1989**, 63, 398.
- [5] M. Guthrie, C. A. Tulk, C. J. Benmore, J. Xu, J. L. Yarger, D. D. Klug, J. S. Tse, H. K., Mao, R. J. Hemley, *Phys. Rev. Lett.* **2004**, 93, 115502.
- [6] P. S. Salmon, J. W. E. Drewitt, D. A. J. Whittaker, A. Zeidler, K. Wezka, C. L. Bull, M. G. Tucker, M. C. Wilding, M. Guthrie, D. Marrocchelli, *J. Phys.: Condens. Matter* **2012**, 24, 415102.
- [7] X. Hong, M. Newville, T. S. Duffy, S. R. Sutton, M. L. Rivers, *J. Phys.: Condens. Matter* **2014**, 26, 035104.
- [8] E. Ohtani, M. Maeda, *Earth Planet. Sci. Lett.* **2001**, 193, 69.
- [9] V. V. Brazhkin, A. G. Lyapin, K. Trachenko, *Phys. Rev. B* **2011**, 83, 132103.
- [10] X. Hong, L. Ehm, T. S. Duffy, *Appl. Phys. Lett.* **2014**, 105, 081904.
- [11] X. Hong, M. Newville, T. S. Duffy, S. R. Sutton, M. L. Rivers, *J. Phys.: Condens. Matter* **2013**, 26, 035104.
- [12] X. Hong, G. Shen, V. B. Prakapenka, M. Newville, M. L. Rivers, S. R. Sutton, *Phys. Rev. B* **2007**, 75, 104201.
- [13] X. Hong, G. Shen, V. B. Prakapenka, M. L. Rivers, S. R. Sutton, *Rev. Sci. Instrum.* **2007**, 78, 103905.
- [14] X. Hong, M. Newville, V. B. Prakapenka, M. L. Rivers, S. R. Sutton, *Rev. Sci. Instrum.* **2009**, 80, 073908.
- [15] R. Ingalls, E. D. Crozier, J. E. Whitmore, A. J. Seary, J. M. Tranquada, *J. Appl. Phys.* **1980**, 51, 3158.
- [16] J. J. Rehr, J. J. Kas, F. D. Vila, M. P. Prange, K. Jorissen, *Phys. Chem. Chem. Phys.* **2010**, 12, 5503.
- [17] J. D. Jorgensen, *J. Appl. Phys.* **1978**, 49, 5473.
- [18] G. Spiekermann, M. Harder, K. Gilmore, P. Zalden, C. J. Sahle, S. Petitgirard, M. Wilke, N. Biedermann, C. Weis, W. Morgenroth, J. S. Tse, E. Kulik, N. Nishiyama, H. Yavaş, C. Sternemann, *Phys. Rev. X* **2019**, 9, 011025.
- [19] M. Vaccari, G. Aquilanti, S. Pascarelli, O. Mathon, *J. Phys.: Condens. Matter* **2009**, 21, 145403.
- [20] M. Baldini, G. Aquilanti, H. K. Mao, W. Yang, G. Shen, S. Pascarelli, W. L. Mao, *Phys. Rev. B* **2010**, 81, 024201.
- [21] Q. Mei, S. Sinogeikin, G. Shen, S. Amin, C. J. Benmore, K. Ding, *Phys. Rev. B* **2010**, 81, 174113.
- [22] J. W. E. Drewitt, P. S. Salmon, A. C. Barnes, S. Klotz, H. E. Fischer, W. A. Crichton, *Phys. Rev. B* **2010**, 81, 014202.
- [23] K. Wezka, P. S. Salmon, A. Zeidler, D. A. J. Whittaker, J. W. E. Drewitt, S. Klotz, H. E. Fischer, D. Marrocchelli, *J. Phys.: Condens. Matter* **2012**, 24, 502101.
- [24] Y. Kono, C. Kenney-Benson, D. Ikuta, Y. Shibazaki, Y. Wang, G. Shen, *Proc. Natl. Acad. Sci. USA* **2016**, 113, 3436.
- [25] X. Du, J. S. Tse, *J. Phys. Chem. B* **2017**, 121, 10726.
- [26] K. Shiraki, T. Tsuchiya, S. Ono, *Acta Crystallogr., Sect. B* **2003**, 59, 701.
- [27] H. K. Mao, J. Xu, P. M. Bell, *J. Geophys. Res.: Solid Earth* **1986**, 91, 4673.
- [28] B. Ravel, M. Newville, *J. Synchrotron Radiat.* **2005**, 12, 537.
- [29] M. Newville, *J. Synchrotron Radiat.* **2001**, 8, 96.
- [30] X. Hua, X. Chen, W. A. Goddard, *Phys. Rev. B* **1997**, 55, 16103.
- [31] G. Paolo, B. Stefano, B. Nicola, C. Matteo, C. Roberto, C. Carlo, C. Davide, L. C. Guido, C. Matteo, D. Ismaila, C. Andrea Dal, G. Stefano de, F. Stefano, F. Guido, G. Ralph, G. Uwe, G. Christos, K. Anton, L. Michele, M.-S. Layla, M. Nicola, M. Francesco, M. Riccardo, P. Stefano, P. Alfredo, P. Lorenzo, S. Carlo, S. Sandro, S. Gabriele, P. S. Ari, S. Alexander, U. Paolo, M. W. Renata, *J. Phys.: Condens. Matter* **2009**, 21, 395502.